

**RESPONSE OF THE GDACS SYSTEM TO THE TOHOKU EARTHQUAKE AND
TSUNAMI OF 11 MARCH 2011**

Annunziato, G. Franchello, T. De Groeve

EC-Joint Research Centre (EC-JRC), Italy

(Presented at 5th Tsunami Symposium of Tsunami Society International (ISPRA-2012) 3-5 Sept. 2012, at EU-Joint Research Centre, Ispra, Italy)

ABSTRACT

The Tohoku Tsunami of 11 March 2011 was successfully identified and classified as Red alert by the GDACS system only when reliable and more correct estimations of the originating event have been provided to the system by the international seismological networks. Nevertheless the early analysis of the event by the comparison of the scenario calculations with the sea level could give important information on the real extent and impact of the Tsunami. The paper describe the response of the GDACS system and identify the lessons learned that determined changes in the logic and the procedures of the Tsunami calculations strategy.

Keywords: *Early Warning Systems, Tsunami, Propagation, Inundation, Alerting*

1. INTRODUCTION

A large earthquake occurred off shore the Pacific coast of Tohoku, Japan (38.1035°N , 142.861°E , M 9.0 at 5:46:18 UTC on March 11, 2011, and generated a large tsunami and caused more than 15000 fatalities and more than 4500 missing, in the east coast of Japan (Fuji et al, 2011). USGS identified the fault mechanism as dipping thrust with strike parallel close to the Japan Trench. The fault movement caused large movements of the earth crust. Continuous measurements of GPS indicated a subsidence of about 1.2 m, close to Central Myagi (Geospatial Information Authority of Japan (GSI)). Several organizations issued Tsunami Alerts for this event; the first was the Japanese Meteorological Agency (JMA) that is in charge in Japan of officially alerting the local communities of potential damaging tsunami events. However the alerting, due to an underestimated initial magnitude of the event, was not indicating the right potential sea level height and was misinterpreted from some of local residents. This paper describes the response of the European Commission's Global Disasters Alerts and Coordination System (GDACS) response to this event.

The Joint Research Centre of the European Commission is operating the Global Disasters Alerts and Coordination System (GDACS, <http://www.gdacs.org>) since 2003. This system, jointly developed by the European Commission and the United Nations, combines existing web-based disaster information management systems with the aim of alerting the international community in case of major sudden-onset disasters and thus facilitating the coordination of international response during the relief phase of each disaster. When new natural disasters events occur, automatic analysis reports are created and sent to users by mail, fax or sms.

As a consequence of the 26 December 2004 tsunami, JRC included the tsunami modeling in the GDACS system in order to improve and complete the automatic reporting system. At the beginning of 2005 a travel time wave propagation model was included (Annunziato 2005). This model calculates the wave arrival times - independently on the initial tsunami wave height. In 2006 a new analytical tool has been developed in order to provide also the wave heights and thus identify the locations with higher risk of tsunami damage (Annunziato, 2007). The model is based on the SWAN propagation code (Mader, 2004), surrounded by a series of systems to automatically react to events and initialize and post-process the code calculations.

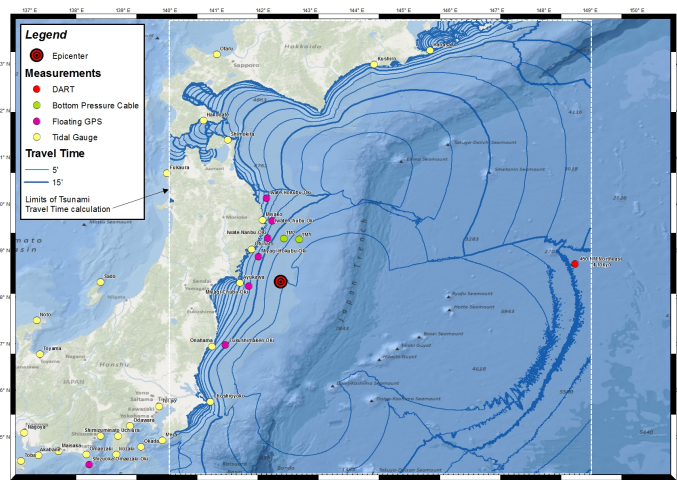


Figure 1 – Identification of the epicenter and several sea level measurements in Japan. The blue curves represent the travel time isochrones each 5 min.

When a potential tsunami occurs (from an earthquake with magnitude greater than 6.5, Richter scale) with epicenter under the water or close to the shoreline (i.e. so that part of the deformation occurs under water), an estimate of the potential consequences of the event is performed and, if the estimated height exceeds certain threshold, an alert is issued and sent to the registered users of the system (20,000 as of July 2012). The initial estimate is based on a pre-calculated scenario composed of 136,000 calculations covering all the potential tsunami sources based on historical catalogs. The epicenters have been obtained creating a grid of 10,168 locations at distance 0.5 min each other, around the historical events and performing 13 calculations, from 6.5 to 9.5 for every 0.25 min. The initial fault in the Mod 1 database is a simple co-sinusoidal function with maximum height equal to the maximum expected deformation for that magnitude and as such it may be considered as a worst-case scenario. A new database is in preparation considering the Okada model for the deformation and historical fault mechanisms.

2. THE GDACS SYSTEM

The Global Disaster Alert and Coordination System (GDACS), is a web-based platform that combines existing web-based disaster information management systems with the aim to alert the international community in case of major sudden-onset disasters and to facilitate the coordination of international response during the relief phase of disaster. GDACS is jointly developed by the JRC and the United Nations Office for Coordination of Humanitarian Affairs (OCHA). (De Groeve et al., 2006, De Groeve, 2007). GDACS comprises of three elements: 1) Web based automatic alert notifications and impact estimations for earthquakes, tsunamis, tropical cyclones, volcanic eruptions and floods. 2) A community of emergency managers and emergency operation centers in responding and disaster-prone countries and disaster response organizations worldwide. 3) Automatic information exchange in web-based disaster information systems. (De Groeve et al., 2009).

The GDACS portal has been built at the Joint Research Centre and available at <http://www.gdacs.org>. It has integrated GDACS compliant information sources and offers a way to register for alert services by email, fax, SMS and/ or RSS as provided by GDACS components. GDACS has 20,000 active users of 184 countries. It has alert and monitoring system for earthquakes and tsunamis, tropical cyclones, volcanic eruptions and floods (De Groeve et al., 2006).

GDACS tsunami alert calculations are triggered by earthquakes that occur in or near water. The logic for the tsunami alert is based on (1) the magnitude and location of the earthquake, (2) the depth of the earthquake, (3) the maximum wave height at any coast reach by the tsunami. The first two parameters are used to look up a tsunami wave height calculation in the JRC Tsunami Database (containing over 132,000 scenarios). For each earthquake of magnitude exceeding 6.5 which occurred in a location under water or close to the shoreline, the tsunami database is queried for the closest matching scenario. Scenarios have been calculated for 10,180 locations covering tsunamigenic regions (from NOAA database) for magnitudes ranging from 6.5M to 9.5M with steps of 0.25M for a total of 136,000 scenarios. If a scenario is available, the maximum wave height at a coast is retrieved. The alert color depends on the maximum wave height according to the following table:

Height (m)		Alert Level
Min	Max	
0	1	Green
1	3	Orange
3		Red

If no scenario has been pre-calculated (only very few cases), the IOC alert matrix is used, based only on earthquake magnitude. This fallback routine, although widely used in tsunami warning centers, results in too many false alerts, therefore the first method is preferred (GDACS, 2010). In any case, after every event - if the scenario exists or not - an automatic online calculation is performed that is useful for a quick analysis but is not useful for the alerting, as the results are available only 20-30 min later.







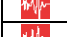
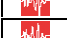




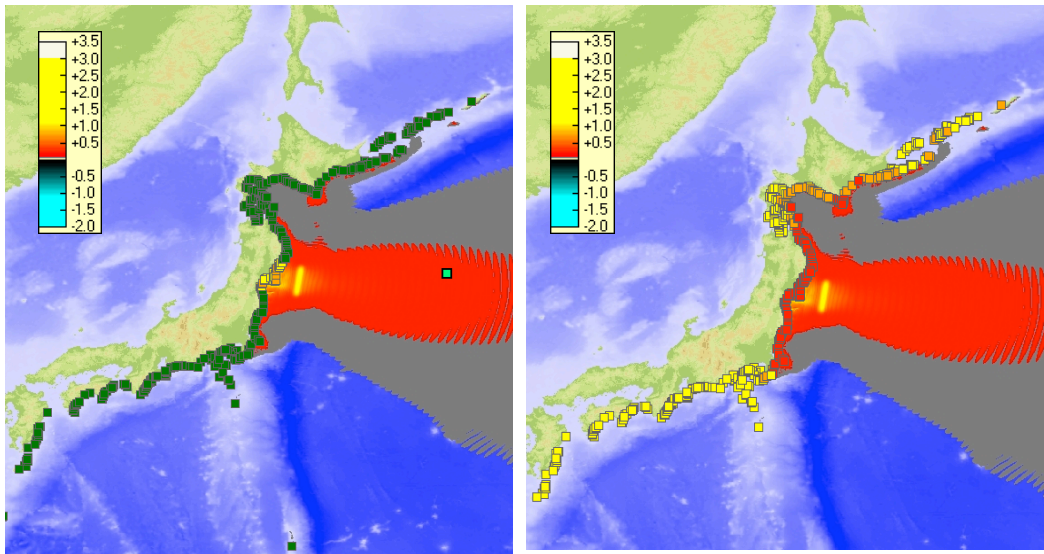
Alert color	Magnitude and depth	Tsunami risk (max height)	Delay	Source
	7.9M, 24.4km	2.1m (at 06:18)	00:20	NEIC
	7.9M, 10.0km	1.8m (at 06:29)	00:20	NEIC
	8.8M, 24.4km	8.6m (at 06:21)	00:42	NEIC
	7.9M,10km	1.8m (at 06:29)	00:43	JMA
	8.8M, 24.4km	8.6m (at 06:21)	00:46	NEIC
	8.8M, 24.4km	8.6m (at 06:21)	00:48	NEIC
	8.8M, 24.4km	8.6m (at 06:21)	00:50	NEIC
	8.4M, 10.0km	5.2m (at 06:22)	02:22	JMA
	8.8M, 24.4km	8.6m (at 06:21)	00:53	NEIC
	8.8M, 10.0km	8.1m (at 06:25)	04:02	JMA
	8.9M, 24.4km	11.9m (at 06:15)	01:08	NEIC
	9.0M, 32.0km	11.6m (at 06:15)	3d	NEIC

Table I – timeline of the events detected by GDACS and the related automatic

3. TSUNAMI ESTIMATIONS FOR THE 11/3/2011 EVENT

In the case of the Japan event of 11/3/2011, the first estimate was obtained 20 minutes after the event with one introduced by USGS into the JRC system (Table I), with parameters 142.369 longitude, 38.3215 latitude and magnitude 7.9 Mw, depth 24.4 km. The initial calculation adopted by GDACS was the calculation identified by the code DISK3/MAG_800/P1425^P0385^0800 which corresponded, in the logic of the GDACS grid storage format to P1425 or +142.5 longitude, P0385 or +38.5 latitude and 0800 or Magnitude 8. This calculation indicates a maximum height of 2.1 m reduced to 1.62 m due to the depth of 24.4 km, in the location Kamaishi, Japan (Fig.1). This value of maximum height called for an Orange alert, automatically sent out to all GDACS users within 20 and 30 min from the event occurrence.

The analysis of the closer DART (Fig. 3) showed that the peak was reached at 6:17 UTC (i.e. 31 min after the event). Considering the delay in the data collection from the buoy which was in the order of 5 min, we knew that the peak was much higher than the values estimated by the online calculation (green curve in Fig. 3) only at 6:23 UTC. In order to get the right value of height, the curve should be multiplied by a value 14. In Ofunato (Fig. 4) the reading went off-scale and could not be possible to compare with the value of the online calculation.



Online calculation results using the initial values of M 7.9 and depth 24.4 km

Online calculation results when multiplied for a factor 14 (only the locations color code is multiplied)

Fig. 2: Maximum estimated height with the online calculation

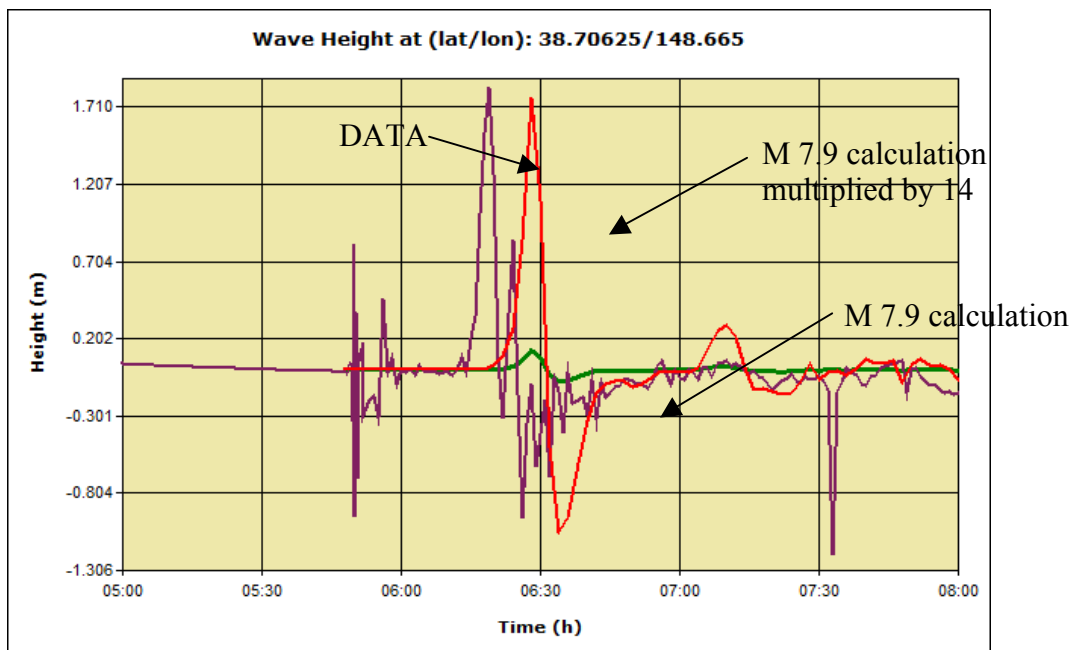


Fig. 3: Sea level estimated on DART 450 NM Northeast of Tokyo (brown curve), compared with the first online calculation (green curve) and the same curve multiplied by a factor 14.

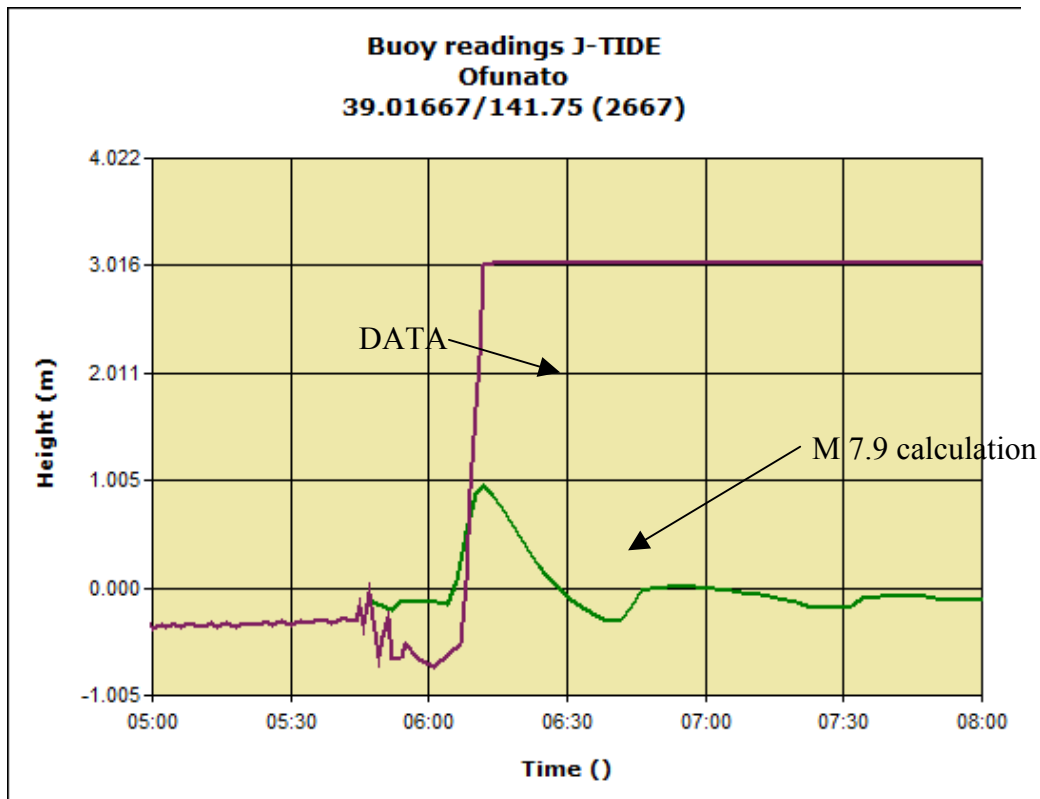


Fig. 4: Sea level estimated on mareograph in Ofunato

The value of 14 in the sea level allowed making the following consideration. Considering that the energy is proportional to the maximum sea level, the above comparison suggests that the energy was 14 times larger than the one corresponding to magnitude 7.9 and the same for the moment magnitude M_0 . The correlation between magnitude and moment magnitude is

$$M_w = \frac{2}{3} \log(M_0) - 10.7$$

If the new Moment Magnitude M_0' 14 times greater than the one for Magnitude 7.9 it means that the new magnitude will be:

$$M_w' = \frac{2}{3} \log(M_0 \times 14) - 10.7 = \frac{2}{3} \log(M_0) - 10.7 + \frac{2}{3} \log(14) = M_w + \frac{2}{3} \log(14) = 7.9 + 0.76 = 8.6$$

This means that the real magnitude had to be at least 8.6 instead of 7.9. Therefore an email to the Monitoring and Information Center (MIC) in Brussels was sent at 6:26 UTC that the estimated magnitude was in the order of 9.0 and that all the possible alerting had to be given.

Few minutes after, at 6:28 UTC we were notified that the magnitude was increased to 8.8. This new estimate of the magnitude called for another re-evaluation of the alert level by GDACS

through the scenario matrix, which now estimated a maximum height of 8.6 m, which meant a Red Alert in the GDACS logic ($h > 3\text{m}$). Therefore a new alert was issued and sent to all the 20,000 GDACS users between 42 and 52 minutes after the event. Much later the event was finally revised to a magnitude 9, after several intermediate revisions; for each revision a new online calculation was performed but no additional alert was sent out because the alert level was not modified and remained Red.

4. POST EVENT CALCULATIONS

Several calculations were performed in the hours after the event in order to identify where the most of the damage occurred.

4.1 Calculations with focal mechanism

A few hours after the event the focal mechanism for this earthquake has been published by USGS and the most probable solution was: depth 32 km, strike 187, dip 14 and rake 681. The width and length assumed for the dislocation area were estimated at 500 km in length and 140 km in width, a rectangular area obtained by available empirical relations of scaling law (Utsu et al., 2001), from magnitude of the earthquake, which can be expressed as follows:

$$\text{Log } L = 0.5 M_w - 1.8$$

$$\text{Log } W = 0.28 L$$

where L , W , M and are fault length (km), width (km) and magnitude (M_w). The results of the comparison with the sea level data is shown in Fig. 5 and shows that the agreement is better than with the scenario calculation but is not yet perfect. The height is underestimated and the peak is wider than in the real case. Also a double peak is not shown. The same plot shows the comparison with the inversion technique that will be described later.

The comparison with the sea level in South Iwate (Fig. 6) shows more clearly that the simple single fault focal mechanism calculation is unable to correctly describe the double sea level increase. Also is not able to show the initial sea level decrease present in the data.

It should be noted that all the measured data have been corrected in order to take into account the initial deformation (Annunziato, 2012).

¹ http://earthquake.usgs.gov/earthquakes/eqinthenews/2011/usc0001xgp/neic_c0001xgp_cmt.php

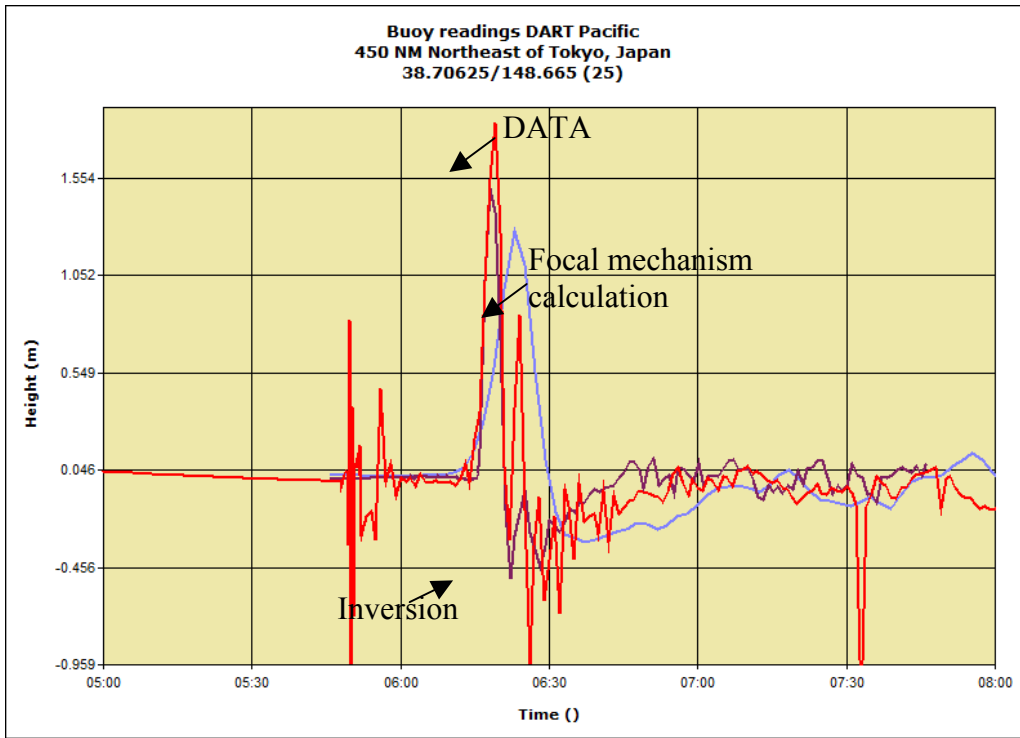


Fig. 5: Sea level estimated on the DART 450 NM NE of Tokyo

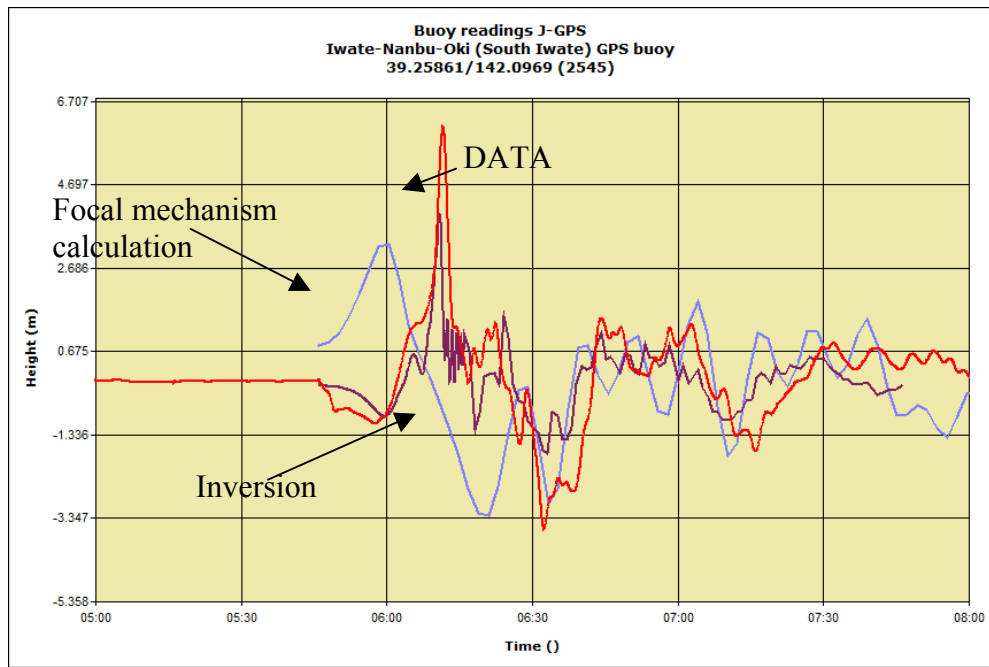


Fig. 6: Sea level estimated on GPS South Iwate

4.2 Inundation Analysis

During the same day of the event we started to perform inundation calculations in order to identify which were the areas potentially mostly affected. The calculations have been performed with the SWAN-JRC code coupled with the Hyflux code for the inundation part (Franchello 2008, 2010 and Franchello et al, 2012).

As the tsunami affected the Eastern coast of Honshu, the analysis subdivided it in three regions of different topography and geographical characteristics. The northern region (1) is mountainous. The tsunami did not reach far inland, but waves were amplified in the many coves. The middle region (2) is flat and densely populated. The southern region (3) is relatively far from the tsunami, but was affected by large aftershocks.

The table below shows the population characteristics of the three regions. Coastal population was identified as living below 5m (using SRTM as a data source for elevation) and within 10km of the coast. Flooded population areas were identified by the HyFlux2 tsunami model. In region 1, the flooded population area is larger than the coastal population because the tsunami was higher than 5m.

	Population		
	Total	Coastal below 5 m	Flooded
Region 1	808 140	69 205	108 215
Region 2	2 578 489	533 755	480 633
Region 3	2 336 596	374 496	187 075
Total	10 249 918	1 143 616	542 071

Flooded area and population are calculated in the three frames (table), validated with remote sensing results in the Sendai area. Figures are compared with the total population in the map extent, and with coastal population living below 5m within 10km of the coast.

Table 2 – Impact of Tsunami Inundation, as estimated the day of the event

From this analysis, the total population living in flooded areas was determined to be more than half a million. This is consistent with reports of people in shelters. While most people are from the Sendai area (region 2), the other regions also have 100,000 and 180,000 affected people.

The most populated region is Miyagi, with the city of Sendai with a population of around 230,000. The relatively flat coastal area caused tsunami waves to increase in height near the shore, reaching more than 15 m. The water inundated up to 4 km inland, fig. 7.

The calculations of JRC match results obtained by interpretation of satellite images. We compared with an analysis of the Colorado Flood Observatory and the National Geospatial

Intelligence Agency (NGA), both published on 13 March 2011. More recent results published by UNOSAT (based on RADARSAT imagery) confirm the accuracy of the JRC analysis. It should be noted that these analyses were performed the same day of the event and therefore could not benefit of the large amount of post Tsunami Survey data that have been produced.

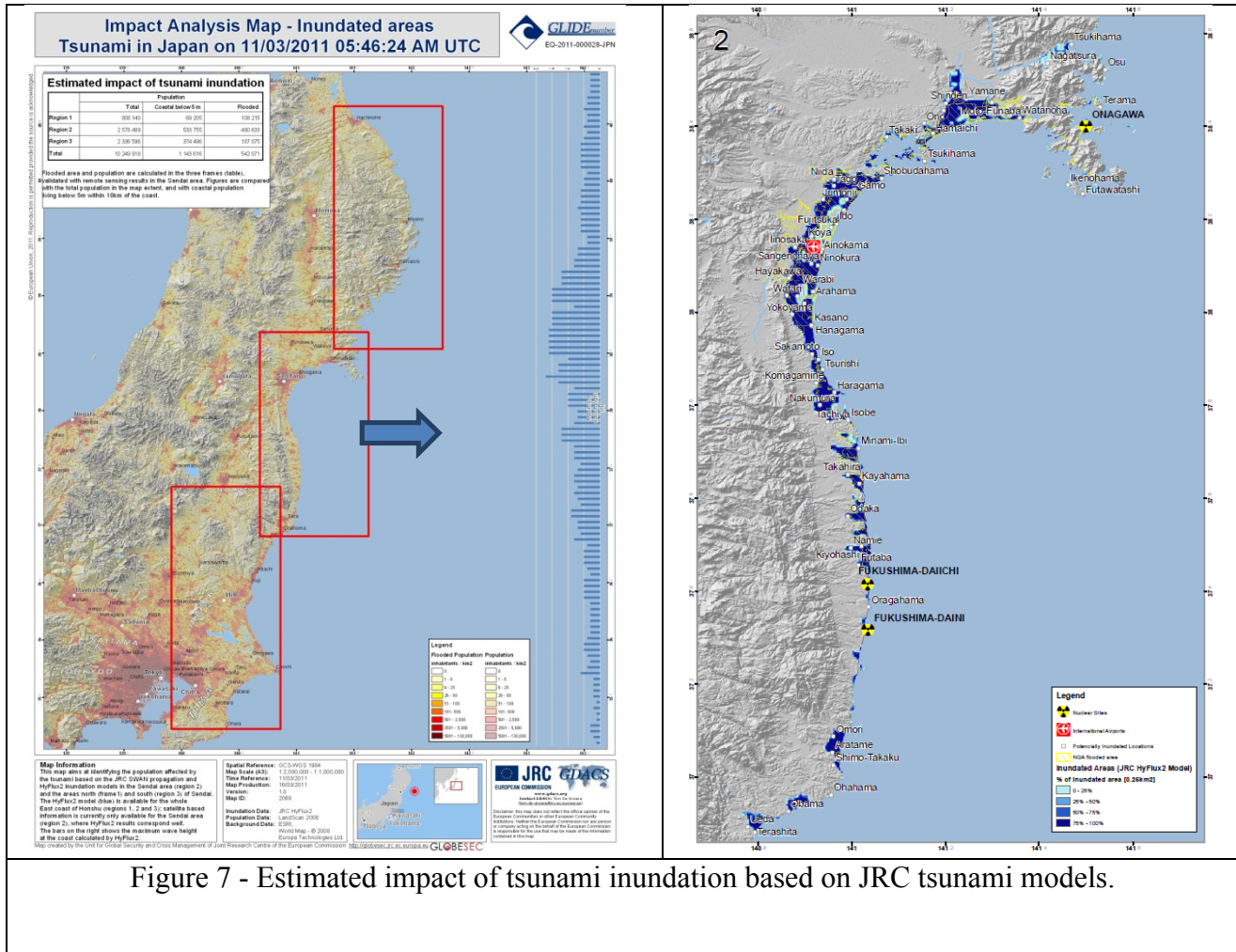


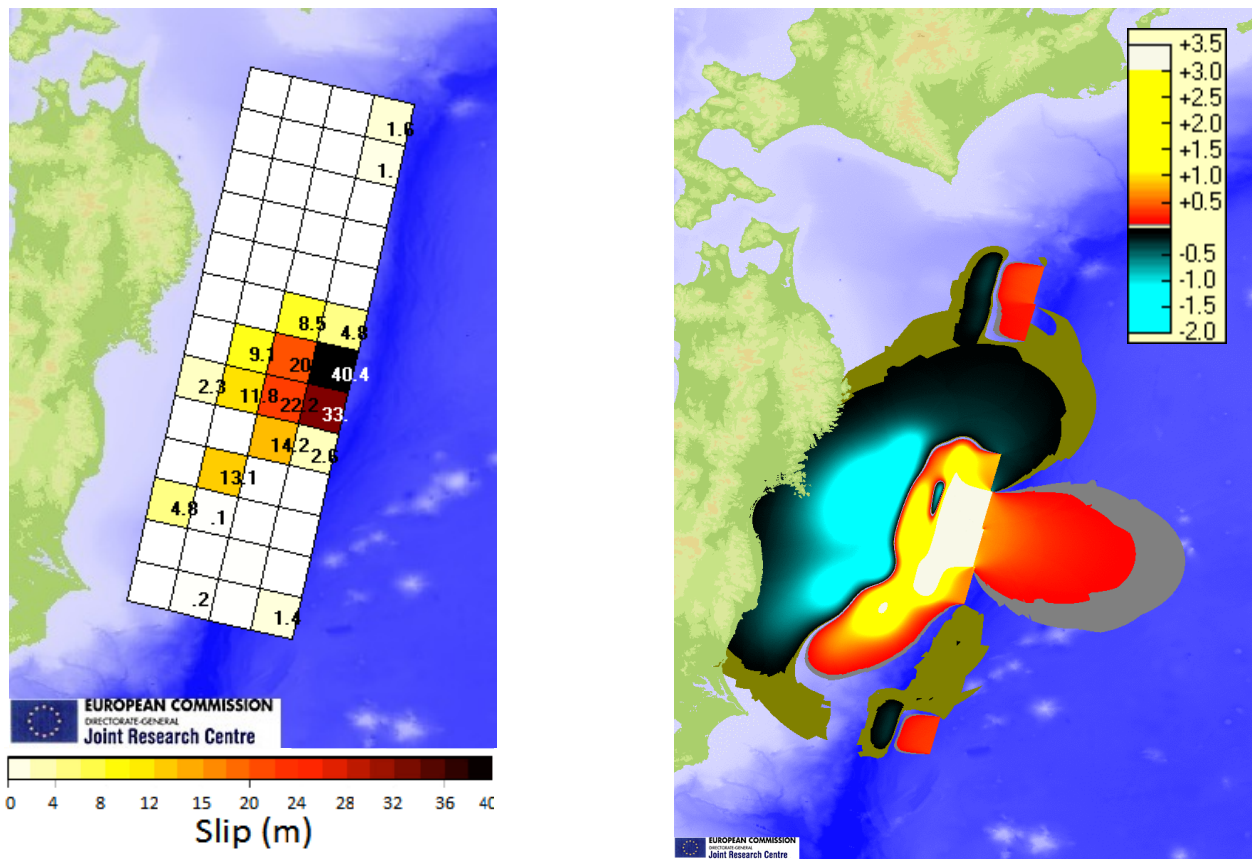
Figure 7 - Estimated impact of tsunami inundation based on JRC tsunami models.

4.3 Source estimation calculations

The large number of sea level measurements in Japan allows performing a very detailed estimation of the initial source (Figure 2); the ones used in this paper are 6 floating GPS, 10 tidal gauges, 2 cable pressure in addition to 3 DART stations provided by NOAA. The floating GPS are buoys equipped with GPS antennas whose signal is analyzed using reference GPS on land to perform a differential measurement; the cable pressure are submarine cables hosting at their end pressure sensor device.

The inversion was performed by creating a matrix of potential unit sources in the area in front of Japan and more specifically around the area that was subject to the aftershock events (Annunziato, 2012). In particular 52 potential faults with unitary slip (1 m) and width/length of 50x50 km have been considered; the additional parameters - strike 193° , dip 14° , slip angle 81° - are from the USGS's W-phase moment tensor solution.

The assumed depth of the faults are 0, 12, 25, 37 km going from the trench towards Honshu island in respect to the reported hypocentral depth. The initial deformation was calculated using the Okada model (1985) and the calculations have been performed using the SWAN-JRC code (Annunziato, 2007) with a grid cell matrix of 1080x1200, cell size of 30 arcsec (0.9 km), GEBCO bathymetry (IOC et al, 2003). In order to compare far distant measurements a coarser nodalization was also used: GEBCO re-sampled at 2 min (3.6 km) and 840x600 grid matrix. All the calculations have been carried out for a 2 hour simulation time.



Estimated slip with JRC Mod 1.0 (50x50 km)

Estimated initial sea level deformation

Fig. 8 – Slip obtained by inversion process and resulting sea level deformation

The form of the slip distribution shows that the fault extension is much smaller than the 500 km assumed for the simple single fault model (note that each square is 50 km and therefore the maximum length is in the order of 200-250 km). The smaller length means also a higher slip in order to respect the energy distribution. Also two sections are evident from the left part of Fig. 8 with a shallower and a much deeper section of the fault. This distinction is the one responsible of the double peaks shown in the data. The comparison of the result of the application of the source distribution obtained by the sea level measurements inversion is shown in the previous figures 4 and 5 and widely described in a paper under review (Annunziato, 2012).

5. DISCUSSION ON THE GDACS RESPONSE

The analysis of the response of the GDACS system allowed drawing some conclusions, which then have led to changes in the automatic procedures.

The early values of the declared magnitudes, in particular for large events like this can be very much affected by the clipping of the instruments and therefore the estimation tend to increase over the time: this was true for Chilean event of 2010 and also for the 2011 event in Japan. This means that it is necessary to check as soon as possible the correspondence between the candidate scenarios with few measured sea levels to eventually correct the proposed magnitude. At this stage we do not find a reliable way to perform automatically this check and therefore we still leave this activity to the operators in charge of such analyses, if any. Nevertheless we are including procedures that allow the operator to react and report the feedback of his/her analysis on the estimates that are shown in the web site online (moderation activity).

The proposed fault mechanisms are very important in order to better describe an event and in some cases (Indonesia, April 2012) can show a completely different mechanism in respect to the one used for the calculations. This is why we are introducing in GDACS an automatic fault mechanism scraping that is able to detect the publication of a fault mechanism online and launch a new calculation that becomes part of the moderation process in the GDACS system.

The inundation calculations should be done automatically following an event and therefore we have now implemented a new calculation strategy so that for each online calculation a series of more and more refined calculations is launched in sequence in order to estimate, within 2 hours from the start of the calculation the inundation extent.

6. CONCLUSIONS

The analysis of the response of the GDACS system to the Tohoku Earthquake has shown that the scenario matrix, which is the base for the alerting system of GDACS, is suitable to identify correctly the sea level impact of tsunamis if correctly initialized with the earthquake parameters. The early comparison with sea level measurements is also able to give indications on the quality of the

candidate scenario automatically selected based on the parameters, which are provided. Much better results can be obtained by the use of the true fault mechanism solutions, which are published a few hours after the event. The use of such data allowed to correctly estimate the sea level inundation in the case of the Tohoku event.

Finally the use of sea level inversion techniques allow to depict much better the real fault extent and its slip distribution, but at the moment it does not seem possible to apply such methods in real time for very detailed source distributions - but is useful to understand the deformation extent.

A number of improvements to the GDACS system are being implemented as a result of the analysis of the Japan event and of other important events that should make the system more reliable and useful for the users community.

REFERENCES

Annunziato, A. (2005). Development and Implementation of a Tsunami Wave Propagation Model at JRC. Proceedings of the International Symposium on Ocean Wave Measurement and Analysis. Fifth International Symposium on Ocean Wave Measurement and Analysis.

Annunziato, A. (2007). The Tsunami Assessment Modelling System by the Joint Research Centre. Science of Tsunami Hazards 26:2, 70-92.

Annunziato, A. (2012). Estimation of the Tsunami Source for the 2011 Tohoku Tsunami – paper under review process.

De Groeve, T.: Global Disaster Alert and Coordination System: More Effective and Efficient Humanitarian Response, Proceedings of the 14th TIEMS Annual Conference, 324-334, Trogir, Croatia, 2007.

De Groeve, T., Peter, T., Annunziato, A. and Vernaccini, L.: Global Disaster Alert and Coordination System, http://www.gdacs.org/documents/2009_GDACS_overview.pdf, 2009.

De Groeve, T., Vernaccini, L. and Annunziato, A.: Modelling Disaster Impact for the Global Disaster Alert and Coordination System, Proceedings of the 3rd International ISCRAM Conference, May 2006, Newark, NJ (USA), 409-417, 2006.

Franchello, G. (2008). Modelling shallow water flows by a High Resolution Riemann Solver. JRC Scientific and Technical Reports. EUR 23307 EN 34p.

Franchello, G. (2010). Shoreline tracking and implicit source terms for a well balanced inundation model. International Journal for Numerical Methods in Fluids 63:10, 1123-1146.

Franchello, G. and Annunziato, A. (2012). The Samoa tsunami of 29 September 2009- Early Warning System and Inundation Assessment. *Science of Tsunami Hazards* 31:1, 19-612.

Y. Fujii, K. Satake, S. Sakai², M. Shinohara, T. Kanazawa – ‘Tsunami source of the 2011 off the Pacific coast of Tohoku Earthquake’ – *Letter to Earth Planets Space*, 63, 815–820, 2011

Mader, C. (2004). *Numerical Modeling of Water Waves*. 2nd ed., CRC Press, Boca Raton, Fl. 274p.